Journal of Alloys and Compounds 509 (2011) 421–425

Contents lists available at ScienceDirect

Journal of Alloys and Compounds

journal homepage: www.elsevier.com/locate/jallcom

Room temperature deposition of Al-doped ZnO thin films on glass by RF magnetron sputtering under different Ar gas pressure

Deok Kyu Kim[a,*], Hong Bae Kim[b]

[a] Brain Korea 21 Chungbuk Information Technology Center, Chungbuk National University, Cheongju 361-763, Chungbuk, Republic of Korea
[b] Division of Electronics and Information Engineering, Cheongju University, Cheongju 360-764, Chungbuk, Republic of Korea

ARTICLE INFO

Article history:
Received 23 June 2010
Received in revised form 3 September 2010
Accepted 8 September 2010
Available online 17 September 2010

Keywords:
Al-doped ZnO
Ar gas pressure
RF magnetron sputtering
Oxygen vacancy
Mobility

ABSTRACT

Al-doped ZnO (AZO) thin films were deposited on glass substrates at room temperature by RF magnetron sputtering. The effects of Ar gas pressure on the structural, optical, and electrical properties were investigated. As the Ar gas pressure increased, the resistivities of the AZO thin films increased, the mobilities decreased, and the carrier concentrations were constant. X-ray photoelectron spectroscopy (XPS) showed that higher Ar gas pressures promoted O–Zn bond formation and reduced the number of oxygen vacancies. The reduction in mobility, which increased the resistivity, was attributed to increased lattice scattering by the oxygen atoms. In AZO thin films deposited at room temperature, the conduction characteristics are primarily influenced by the mobility.

1. Introduction

Al-doped ZnO (AZO) thin films have high visible transparency and electrical conductivity, so they are of increasing interest for fabricating transparent electrodes for light emitting diodes, solar cells, and transparent thin film transistors [1–4]. The use of a glass substrate is indispensable in the application of these films to transparent devices, but imposes an upper limit on deposition temperatures; it is necessary to prepare AZO thin films at low temperatures such as room temperature. Magnetron sputtering is the preferred technique because of its potential for room-temperature processing [5]. Many researchers have therefore tried to produce high quality AZO thin films deposited at room temperature by magnetron sputtering [6–9]. Lee and Song [8] have reported the deposition of AZO films at room temperature by RF sputtering with a bias voltage. Chen et al. [9] have successfully fabricated AZO thin films at room temperature with oxygen control. However, there have been no previous reports showing the effects of Ar gas pressure on the properties of AZO thin films deposited at room temperature by RF magnetron sputtering.

In this study, AZO thin films were deposited at room temperature by RF magnetron sputtering at various Ar gas pressures, and analyzed comparatively by structural, optical, and electrical measurements. In addition, chemical bonding changes in the AZO thin films were investigated to get a better understanding of the measured characteristics of the AZO thin films.

2. Experimental procedure

AZO thin films have been prepared by RF magnetron sputtering from an oxide ceramic target consisting of 98 wt% ZnO and 2 wt% Al_2O_3 with 3 in. diameter. The substrates were corning 1737 glasses, which were degreased in organic solution, rinsed in deionized water and blown dry in N_2 gas before they were loaded into the chamber. High purity Ar was introduced through mass flow controller after the vacuum chamber was evacuated below 2.0×10^{-6} Torr. The Ar gas pressure was varied to 1×10^{-3} Torr, 1.5×10^{-3} Torr, and 2×10^{-3} Torr. The process pressure was kept at 2.0×10^{-2} Torr and the sputtering power was 25 W. The AZO thin films with thickness of 250 nm were deposited without intentional heating.

The crystal structure of the different AZO thin films was analyzed by X-ray diffraction (XRD) by using the nickel filtered Kα emission line ($\lambda = 1.5406$ Å) of copper in a Phlilips X'pert. The surface morphology of AZO thin films was examined using a PUCOTECH atomic force microscope (AFM) under the non-contact mode. Optical measurement of AZO-coated substrate was done with unpolarized light at normal incidence in the wavelength range from 250 nm to 1000 nm, with JASCO UV/VIS/NIR spectrophotometer. Hall measurement for the resistivity, carrier concentration and mobility determination were accomplished at room temperature in an ECOPIA HMS-3000. The chemical bonding structures were investigated using an X-ray photoelectron spectroscopy (XPS) in THERMO VG SCIENTIFIC MultiLab2000.

3. Results and discussion

The XRD spectra for AZO thin films deposited on glass at room temperature are shown in Fig. 1. Fig. 1 illustrates that (0 0 2) was the prominent plane for AZO thin film prepared by this method. All of AZO thin films have a strong diffraction peak of (0 0 2) at 2θ location of ∼34.4°, which are very close to that of the standard ZnO

---

[*] Corresponding author. Tel.: +82 43 261 3327; fax: +82 43 229 8461.
E-mail address: maruchi111@naver.com (D.K. Kim).

0925-8388/$ – see front matter © 2010 Elsevier B.V. All rights reserved.
doi:10.1016/j.jallcom.2010.09.047

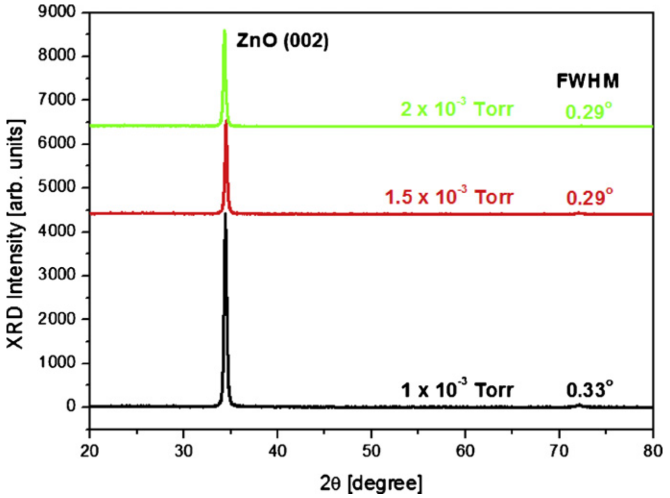

Fig. 1. XRD patterns corresponding to AZO thin films with various Ar gas pressure. All of samples have a *c* plane preferred orientation.

crystal (34.45°), independent of the Ar gas pressure. No Al_2O_3 phase was detected from the XRD patterns. This may be due to Al replacing zinc substitutionally in the hexagonal lattice or Al segregate to the non-crystalline region in the grain boundary [10]. The intensity and the full width at half maximum (FWHM) become weaker and narrower with increasing the Ar gas pressure. The FWHM for AZO thin films prepared at different Ar gas pressure of 1×10^{-3} Torr, 1.5×10^{-3} Torr, and 2×10^{-3} Torr was 0.33°, 0.29°, and 0.29°, indicating the crystallinity improvement of AZO thin films as the Ar gas pressure increased, respectively. This result conflicts with earlier findings. Song [11] and Ikasaki [12], which deposited AZO thin films at high temperature, reported a decrease of FWHM with increasing the Ar gas pressure. Therefore, the opposite result is due to different substrate temperature. The average crystallite size (*D*), which is the length of the crystal in the direction of the d spacing, was calculated using Scherrer's formula [13]:

$$D = \frac{0.9\lambda}{B\cos\theta}$$

where λ is the X-ray wavelength (1.5406 Å), B is the FWHM and θ is the Bragg diffraction angle. The average crystallite size was found to be 25.2 nm (1×10^{-3} Torr), 28.68 nm (1.5×10^{-3} Torr), and 28.67 nm (2×10^{-3} Torr), which increases with the increase of the Ar gas pressure, respectively.

The surface morphology of AZO thin films was revealed by the AFM images as shown in Fig. 2. It can be seen that the root mean square (RMS) roughness and grain size of the AZO thin films increases with increasing of the Ar gas pressure. This result coincides with the previous study to deposit AZO thin films at high temperature. The RMS roughness for Ar gas pressure of 1×10^{-3} Torr, 1.5×10^{-3} Torr, and 2×10^{-3} Torr was 1.47 nm, 2.01 nm, and 2.27 nm, respectively. The reason why the RMS roughness increases is because the energy of particles arriving at the surface decreases with increasing argon pressure, leaving less energy for surface diffuse due to collisions with more atoms [11]. The AZO thin film with a surface roughness of ~2 nm is sufficient to meet the requirement for optical device application. The result of RMS roughness agrees with result of average crystallite size calculated using Scherrer's formula, as shown in Fig. 3.

The dependence of electrical resistivity (ρ), carrier concentration (n), and mobility (μ) on Ar gas pressure is shown in Fig. 4. The results showed that all the films are degenerate doped n-type semiconductor. As Ar gas pressure increases, the electrical resistivity increases, the mobility decreases, and the carrier concentration almost constant. These results show similar electrical properties to those deposited at high temperature except carrier concentration. The lowest electrical resistivity of 3.491×10^{-3} Ωcm, the highest Hall mobility of 4.159 cm/Vs, and the carrier concentration of 4.299×10^{20} cm^{-3} obtained at the Ar gas pressure of 1×10^{-3} Torr. In contrast with a large variation of mobility, the carrier concentration does not show a significant change in AZO thin films prepared at different Ar gas pressure, which indicates that the low resistivity of the AZO thin film prepared at optimal Ar gas pressure is mainly attributed to its high mobility. This conduction behavior shown a different aspect from AZO thin films deposited at high temperature. About this, it will be discussed later.

Fig. 5 shows the transmittance spectra as a function of wavelength in the range 250–1000 nm for AZO thin films. It can be seen

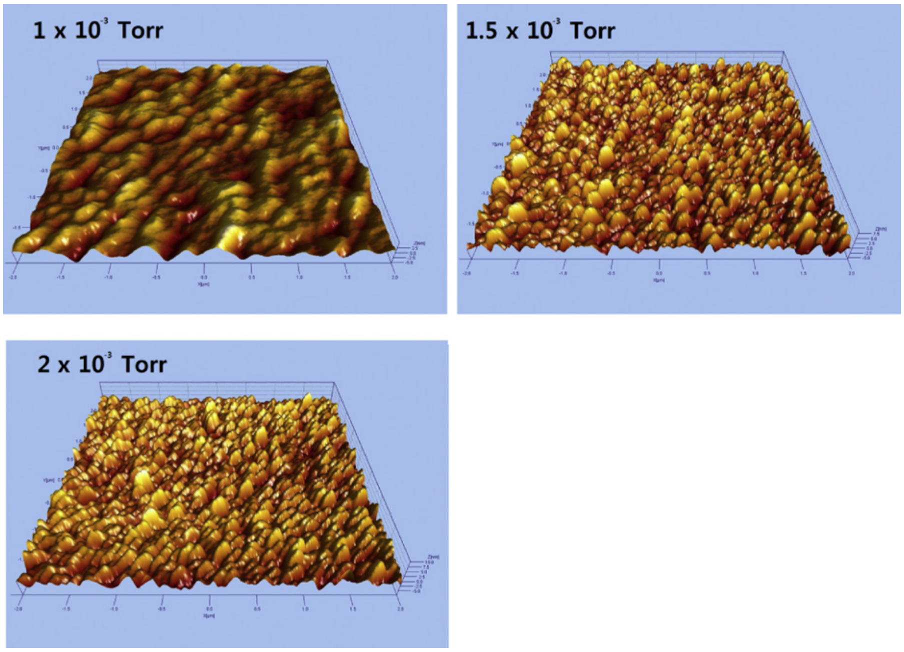

Fig. 2. AFM 3D images of AZO thin films with various Ar gas pressure. Scan area is 2 μm × 2 μm.

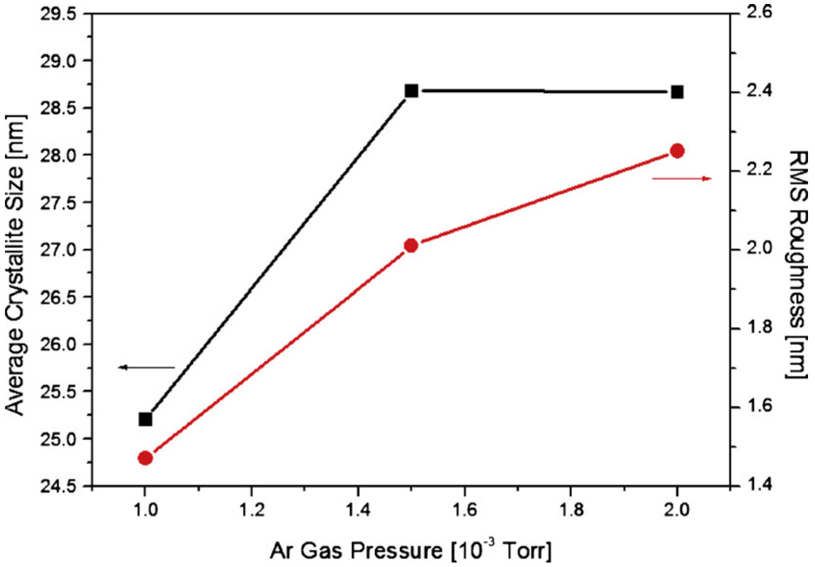

Fig. 3. Average crystallite size calculated from the Scherrer's formula and RMS roughness with various Ar gas pressure.

that the average transmittance in the visible wavelength region is about 82–85% for all the films, which means that the Ar gas pressure does not have a significant effect on the transparency of the films over the visible light wavelength range. However, the short wavelength cut-off in transmittance of AZO thin films has a clear shift towards the long wavelength range with increasing the Ar gas pressure, indicating that the optical energy gap is reduced.

The optical energy gap (E_g) of the thin films can be determined by the extrapolation methods from the absorption spectrum ($\alpha h\nu$) which is given by [14]:

$$\alpha h\nu = C(h\nu - E_g)^{1/2}$$

where C is a constant for direct transition, and $h\nu$ is the photon energy. The absorption coefficient (α) can be calculated from transmittance by the following equation [15].

$$\alpha = \frac{\ln(1/T)}{d}$$

where d is the film thickness of the ZnO thin films. These calculations are illustrated in Fig. 6, where it is observed that the gap energy value decreases as the Ar gas pressure increases in the studied rage, from 3.537 eV to 3.403 eV. Usually, the gap energy of AZO thin films is found higher than that of bulk ZnO material (E_g = 3.37 eV) owing to broadening caused by the Burstein–Moss effect [16]. Also, changes in the gap energy of ZnO thin films have been related to variations in the average crystallite size, the internal stress and the free carrier concentration [16–18]. The shift of the gap energy can be related to the corresponding change in the average crystallite size shown in Fig. 3. Lin [18] and Marotti [19] have already proven for ZnO thin films that the crystallite size affects the optical properties, obtaining higher energy gap for thin films with smaller crystallite size. Such trend is generally observed for the present samples.

The chemical bonding configurations of deposited AZO thin films are an important factor in their structural, optical, and electrical properties. The chemical bonding configurations were investigated by X-ray photoelectron spectroscopy (XPS). The atomic concentrations of the elements present were calculated from the measured peak areas and sensitivity factors of high-resolution XPS spectra [20]. Fig. 7 shows the variations in the

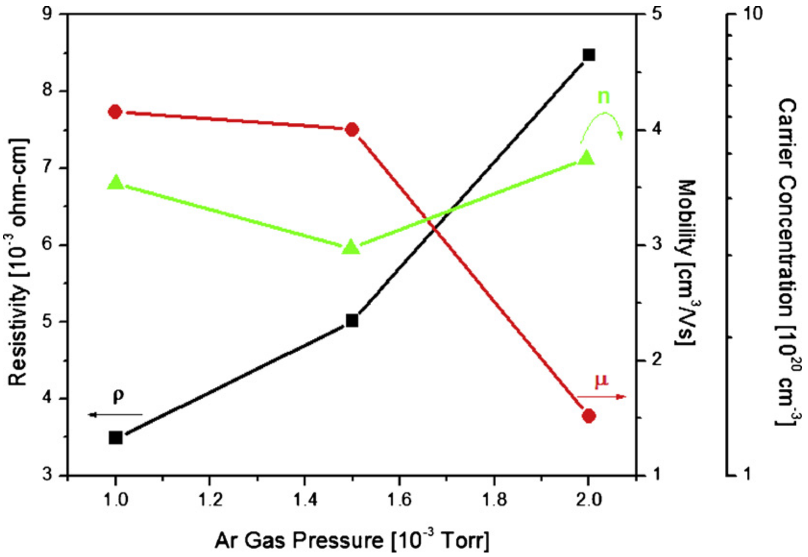

Fig. 4. Resistivity, mobility and carrier concentration as a function of Ar gas pressure.

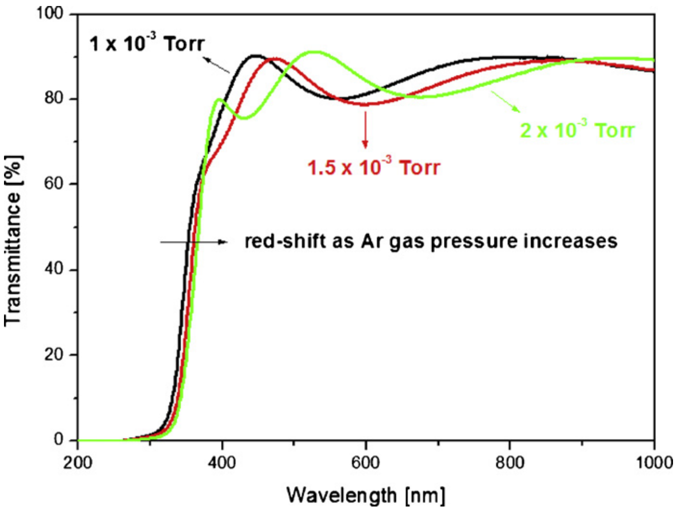

Fig. 5. Optical transmittance as a function of the light wavelength for AZO thin films with various Ar gas pressure.

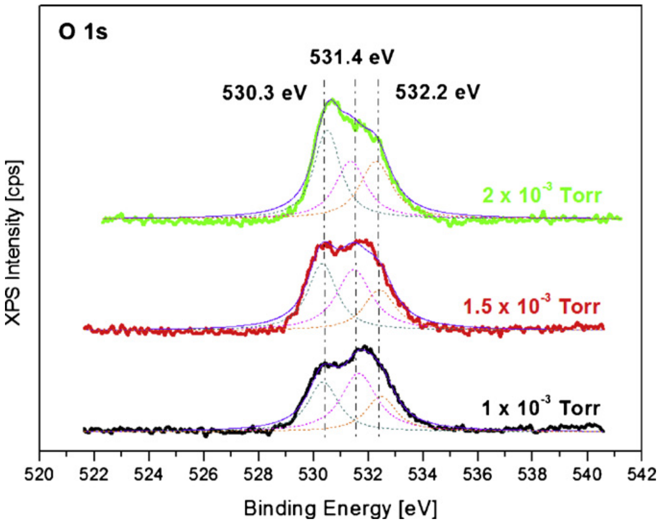

Fig. 8. XPS spectra of O 1 s core levels of AZO thin films with Ar gas pressure.

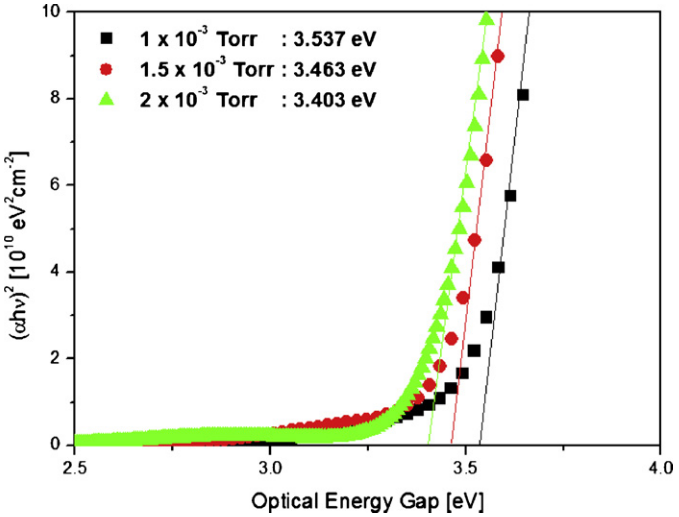

Fig. 6. Band gap energy calculation from the optical transmittance spectra as a function of the light energy for AZO thin films with various Ar gas pressure.

O/(Zn + Al) ratios and the Al content of the AZO thin films as a function of the Ar gas pressure. All of the AZO thin films displayed Zn (or Al) rich compositions, and with increasing Ar gas pressure the O/Zn ratio approached 1, indicating a stoichiometric composition. Zn (or Al) enrichment helps to stabilize AZO thin films under plasma conditions [21]. The Al compositions for Ar gas pressures of 1×10^{-3} Torr, 1.5×10^{-3} Torr, and 2×10^{-3} Torr were 2.37 at%, 3.47 at%, and 3.00 at%, respectively. The resistivity was expected to decrease as the Al composition increased, but this was not borne out by the measured resistivities. This shows that the Al dopant is not the only parameter which affects resistivity. In general, the resistivity of a ZnO thin film is influenced by Zn interstitial atoms or oxygen vacancies [22]. Chemical state changes in the AZO thin films were therefore analyzed by XPS. The Zn $2p_{3/2}$ and Al $2p_{3/2}$ core lines (not shown here) were highly symmetric and centered at 1021.79 ± 0.10 eV and 74 ± 0.10 eV, respectively [23]. No metallic Zn or Al, binding energies 1021.5 eV [24] and 72.7 eV [25], respectively, were observed. This shows that Zn and Al existed only in the oxidized state. The XPS spectra of the O 1 s core level were deconvolved into three components located at 530.3 eV, 531.4 eV, and 532.2 eV (Fig. 8). The low binding energy peak centered at

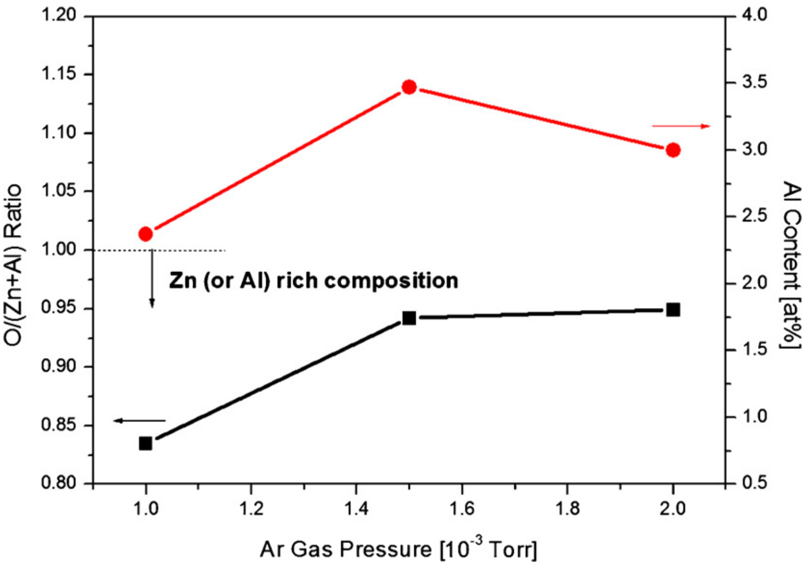

Fig. 7. O/(Zn+Al) ratio and Al content obtained from the XPS measurement with Ar gas pressure.

530.3 eV is attributed to the O 1 s level in the ZnO wurtzite structure surrounded by Zn (or substituted Al) atoms with their full complement of nearest-neighbor O^{2-} ions [26]. The medium binding energy peak at 531.4 eV is associated with O^{2-} ions in the oxygen deficient regions within the ZnO matrix [27]. The high binding energy peak at 532.2 eV is attributed to adsorbed or chemisorbed oxygen species such as O_2, H_2O, or CO due to surface hydroxyl groups [28]. The relative changes in the low and medium binding energy components therefore reveal the degree of O–Zn bonding and oxygen vacancies. The level of O–Zn bonding increases with increasing Ar gas pressure; in contrast, the level of oxygen vacancies significantly decreases. The changes in the number of oxygen vacancies with Ar gas pressure are consistent with the resistivity results. The conduction characteristics of AZO thin films deposited at high temperatures are primarily dominated by electrons generated by O^{2-} vacancies [22]. However, in our samples, the resistivity was affected by the mobility because of the constant carrier concentration, as mentioned above. We therefore concluded that the resistivity increases with decreasing mobility as a result of the reduction in the number of oxygen vacancies, that is, as the Ar gas pressure increases, the number of oxygen vacancies decreases, and the number of oxygen atom in the lattice increases. The lattice scattering therefore increases and the mobility is reduced by the increased lattice scattering. Finally, the reduced mobility increases the resistivity of the AZO thin films. The deconvolution results indicated that the medium energy peak at 531.4 eV became more intense for AZO thin films deposited at lower Ar gas pressures, and that this is beneficial in lowering the film resistivity, whether the number of electrons increases or the mobility increases. We also observed that the crystallinity improved, the average crystallite size increased, and the RMS roughness increased as a result of a reduction in the number of oxygen vacancies and an increase in the number of O–Zn bonds. The experimental results showed that Ar gas pressure is the dominant factor in determining the amounts of O–Zn bonds and oxygen vacancies in AZO thin films, and that mobility plays a major role in the conduction behavior of AZO thin films deposited at room temperature. AZO deposition at lower Ar gas pressures can promote the formation of oxygen vacancies, leading to low resistivity.

4. Conclusion

In this study, AZO thin films with a highly (0 0 2)-preferred orientation were deposited at room temperature, using various Ar gas pressures, by RF magnetron sputtering. Various properties of the AZO films were investigated. The crystallinity, surface roughness, and optical band-gap energy were dependent on the Ar gas pressure. With increasing Ar gas pressure, the resistivity increased and the mobility decreased because of the reduction in the number of oxygen vacancies. We confirmed that mobility is the key parameter in determining the resistivity of AZO thin films at room temperature. AZO thin films deposited at room temperature have satisfactory properties, i.e., low resistivity and high transmittance, for applications in transparent electrodes and optoelectronic devices.

References

[1] T. Minami, Thin Solid Films 516 (2008) 5822.
[2] B.S. Chua, S. Xu, Y.P. Ren, Q.J. Cheng, K. Ostrikov, J. Alloys Compd. 485 (2009) 379.
[3] W. Gao, Z.W. Li, J. Alloys Compd. 449 (2008) 202.
[4] M.H. Huang, S. Mao, H. Feick, H. Yan, Y. Wu, H. Kind, E. Weber, R. Russo, P. Yang, Science 292 (2001) 1897.
[5] H.W. Kim, N.H. Kim, Mater. Sci. Eng. B 103 (2003) 297.
[6] X.B. Zhang, Z.L. Pei, J. Gong, C. Sun, J. Appl. Phys. 101 (2007) 014910.
[7] J.W. Seong, K.H. Kim, Y.W. Beag, S.K. Koh, K.H. Yoon, J. Vac. Sci. Technol. A 22 (2004) 1139.
[8] J.H. Lee, J.T. Song, Thin Solid Films 516 (2008) 1377.
[9] M. Chen, Z.L. Pei, X. Wang, C. Sun, L.S. Wen, Mater. Lett. 48 (2001) 137.
[10] X.T. Hao, L.W. Tan, K.S. Ong, F. Zhu, J. Cryst. Growth 287 (2006) 44.
[11] D. Song, A.G. Aberle, J. Xia, Appl. Surf. Sci. 195 (2002) 291.
[12] Y. Igasaki, H. Kanma, Appl. Surf. Sci. 169–170 (2001) 508.
[13] B.D. Cullity, Elements of X-ray Diffraction, Addison-Wesley, 1978, 102.
[14] J.I. Pankove, Optical Processes in Semiconductors, Dovr, New York, 1976.
[15] H.R. Fallah, M. Ghasemi, A. Hassanzadeh, H. Steki, Mater. Res. Bull. 42 (2007) 487.
[16] M. Suchea, S. Christoulakis, N. Katsarakis, T. Kitsopoulos, G. Kiriakidis, Thin Solid Films 515 (2007) 6562.
[17] R.E. Marotti, P. Giorgi, G. Machado, E.A. Dalchiele, Sol. Energy Mat. Sol. Cells 90 (2006) 2356.
[18] H.P. He, F. Zhuge, Z.Z. Ye, L.P. Zhu, F.Z. Wang, B.H. Zhao, J.Y. Huang, J. Appl. Phys. 99 (2006) 023503.
[19] S.S. Lin, J.L. Huang, Surf. Coat. Technol. 185 (2004) 222.
[20] X.Q. Wei, B.Y. Man, M. Liu, C.S. Xue, H.Z. Zhuang, C. Yang, Physica B 388 (2007) 145.
[21] H.C. Wewller, R.H. Mauch, G.H. Bauer, Sol. Energy Mater. Sol. Cells 27 (1992) 217.
[22] L. Li, L. Fang, M. Chen, Rare Met. 26 (2007) 247.
[23] L. Li, L. Fang, X.J. Zhou, Z.Y. Liu, I. Zhao, S. Jiang, J. Electron Spectrosc. Relat. Phenom. 173 (2009) 7.
[24] M.N. Islam, T.B. Ghosh, K.L. Chopra, H.N. Acharya, Thin Solid Films 280 (1996) 20.
[25] C.D. Wagner, W.M. Riggs, L.E. Davis, J.F. Moulder, G.E. Muilenberg, Handbook of X-ray Photoelectron Spectoscopy, PerkinElmer Corporation, Eden Prairie, MN, 1979, pp. 50–51.
[26] N.S. Ramgir, I.S. Mulla, V.K. Pillai, J. Phys. Chem. B 110 (2006) 3995.
[27] J.C. Fan, J.B. Goodenough, J. Appl. Phys. 48 (1977) 3524.
[28] N.S. Ramgir, D.J. Late, A.B. Bhise, M.A. More, I.S. Mulla, D.S. Joag, K. Vijayamohanan, J. Phys. Chem. B 110 (2006) 18236.